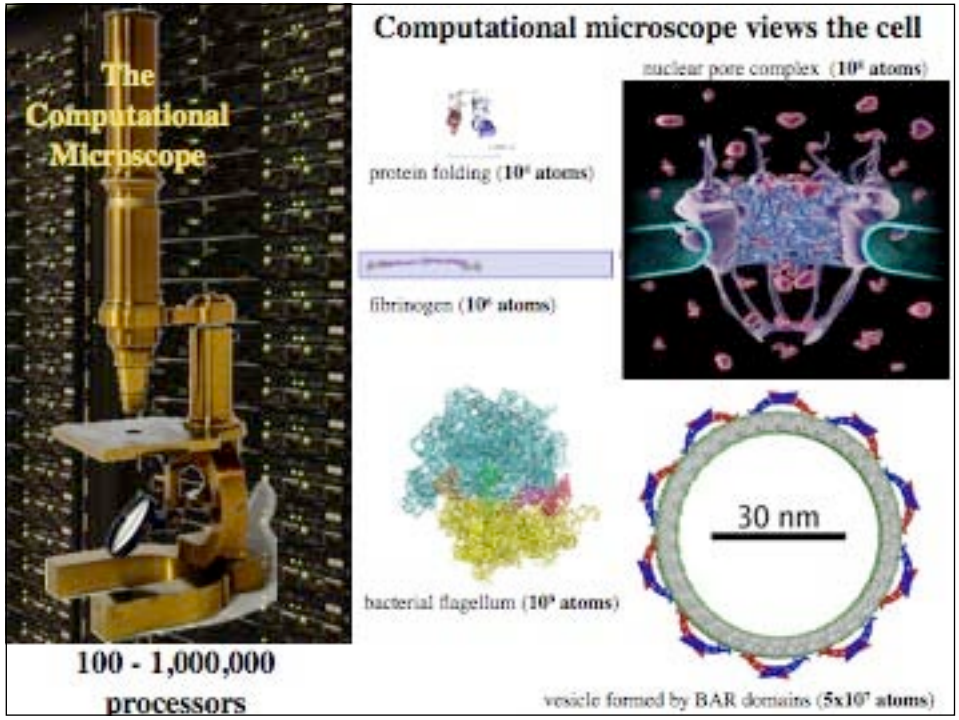
The Computational Microscope
Computational microscope views the cell
nuclear pore complex (10⁸ atoms)
protein folding (10⁴ atoms)
fibrinogen (10⁵ atoms)
30 nm
bacterial flagellum (10⁶ atoms)
100 - 1,000,000 processors
vesicle formed by BAR domains (5x10⁷ atoms)

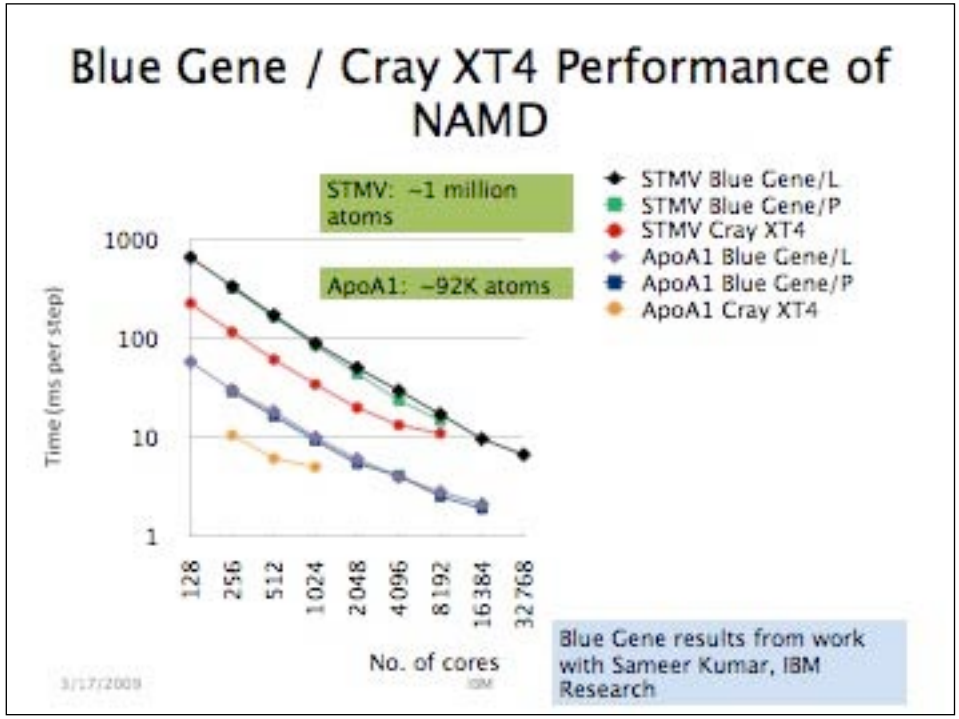
Blue Gene / Cray XT4 Performance of NAMD
STMV: ~1 million atoms
ApoA1: ~92K atoms
STMV Blue Gene/L
STMV Blue Gene/P
STMV Cray XT4
ApoA1 Blue Gene/L
ApoA1 Blue Gene/P
ApoA1 Cray XT4
Time (ms per step)
1000
100
10
1
128
256
512
1024
2048
4096
8192
16384
32768
No. of cores
Blue Gene results from work with Sameer Kumar, IBM Research
3/17/2009

PME Optimized by DCMF Many-to-many

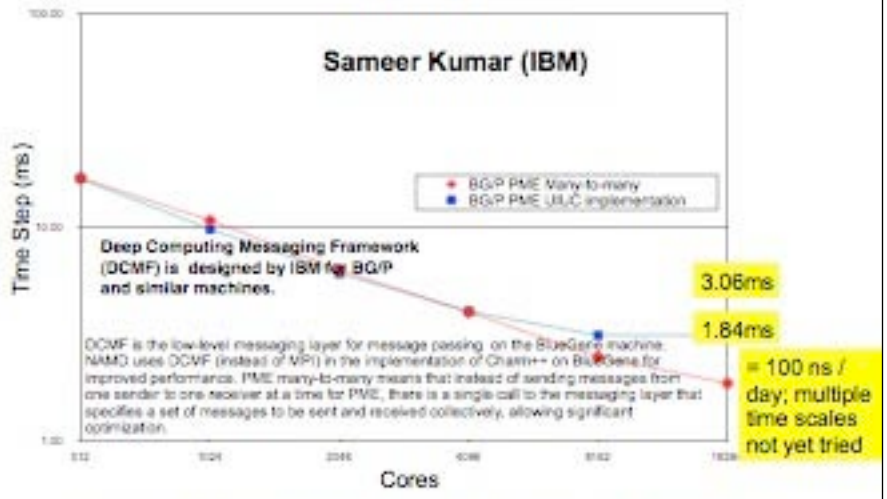

92K Atom APoA1 Benchmark with PME every step in Quad Mode (4 cores used)

Viewing the 10 μs Folding of a Protein

- Solvated system is ~30,000 atoms
- Simulated in NAMD using CHARMM22/ CMAP
- ~100 ns/day on 329 processors
- Starting conformations either fully extended or thermally denatured
- Three independent WT simulations done
- Six mutant simulations
- Altogether over 50 μs of simulation
- Simulations of WW domain reveal deficit of force field

Protein dynamics in cells go out to a millisecond and longer. We recently increased computational time scales from 100 ns to 60 microseconds!

Over **50 microsecond** of protein folding

WT villin head piece; exp 4 μs, sim 6 μs

Folding WT villin *in silico*

Three folding simulations reach native state within 5-8 μs

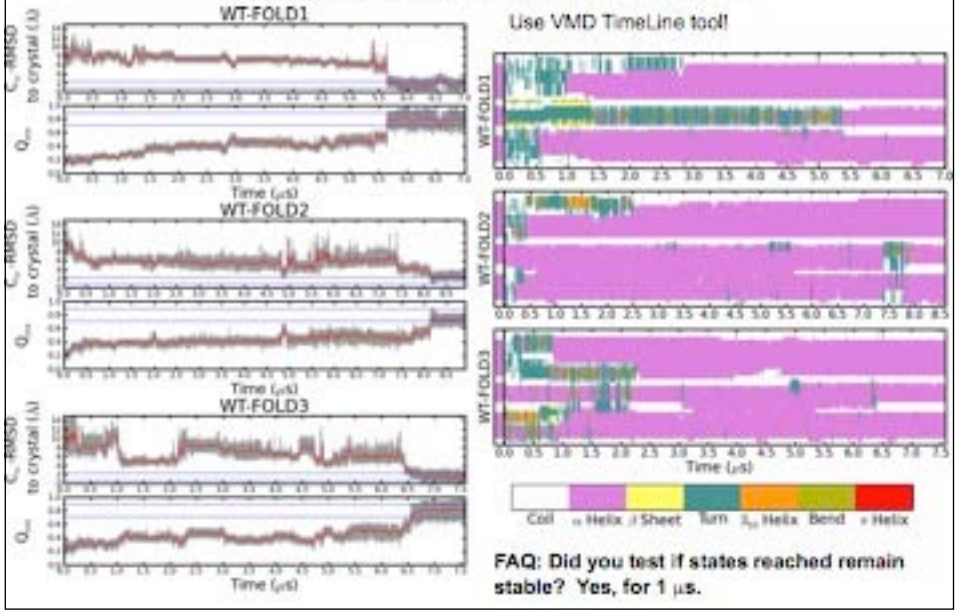

Use VMD TimeLine tool!

FAQ: Did you test if states reached remain stable? Yes, for 1 μs.

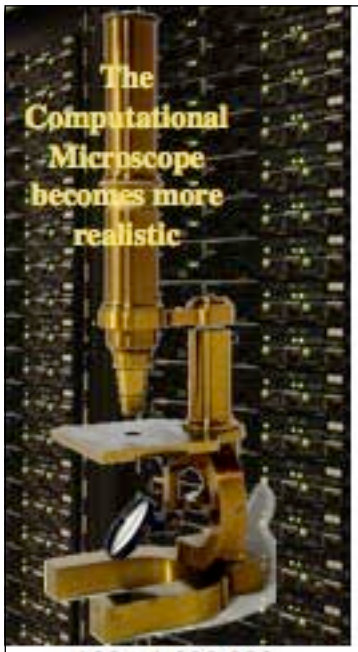

100 - 1,000,000 processors

Implementing Polarizable Force Fields into NAMD

Atomic polarizability not yet accounted for in modeling. Respective force fields are being developed; here the fluctuating charge model of Brooks et al.

Polarizable water; fluct. charge

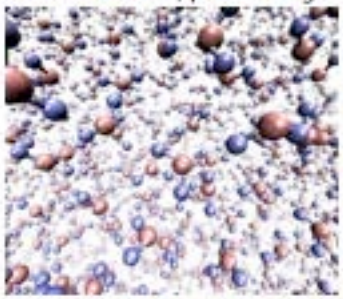

Goal: Realize polarizable force fields in our modeling program effectively.

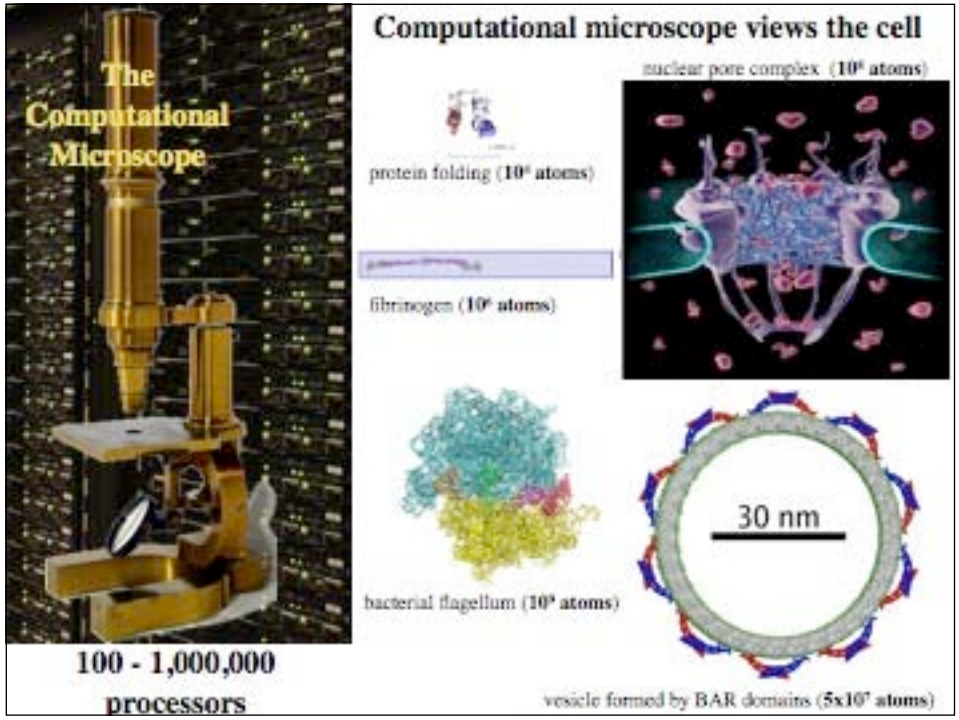

Inspecting the mechanical Strength of a blood clot

Collaborator: Bernard C. Lim (Mayo Clinic College of Medicine)

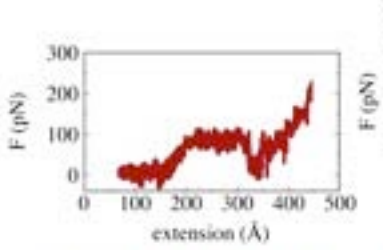

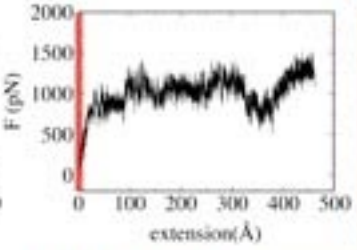

20ns SMD Simulation of fibrinogen, *1.06 million atoms, 1.2 ns/day with pencil decomposition, 15 days on PSC XT3 Cray (1024 processors)*

B. Lim, E. Lee, M. Sotomayor, and K. Schulten. **Molecular basis of fibrin clot elasticity.** *Structure*, 16:449-459, 2008.

A Blood Clot

Red blood cells within a network of fibrin fibers, composed of polymerized fibrinogen molecules.

NIH Center for Research Resources

Inspecting the mechanical Strength of a blood clot

Collaborator: Bernard C. Lim (Mayo Clinic College of Medicine)

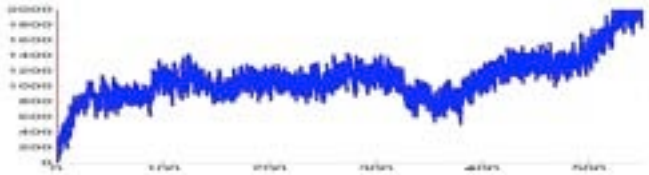

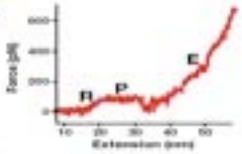

20ns SMD Simulation of fibrinogen, *1.06 million atoms, 1.2 ns/day with pencil decomposition, 15 days on PSC XT3 Cray (1024 processors)*

B. Lim, E. Lee, M. Sotomayor, and K. Schulten. **Molecular basis of fibrin clot elasticity.** *Structure*, 16:449-459, 2008.

A Blood Clot

Red blood cells within a network of fibrin fibers, composed of polymerized fibrinogen molecules.

NIH Center for Research Resources

Petascale simulations will Permit Sampling

For Example Carrying out a Second Simulation Required by a Referee

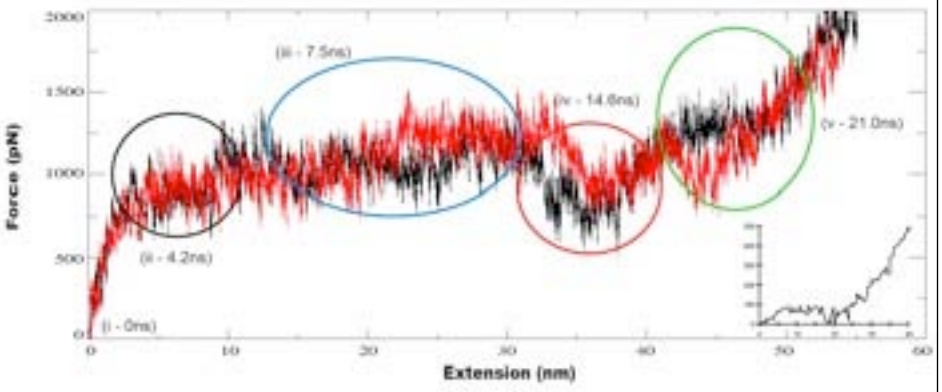

Simulation of soft, tertiary structure elasticity of titin

This type of elasticity was fist discovered in ankyrin:

Ankyrin - tertiary structure spring at weak force (25 pN)

340,000 atom simulation of 24 repeat ankyrin

simulated

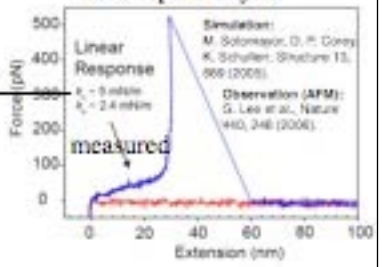

Ankyrin - secondary structure spring at large force

simulated

Experiment: L. Li, S. Wetzel, A. Pluckthun, and J. M. Fernandez, Biophys. J. 90, L30–L32, 2006.

measured

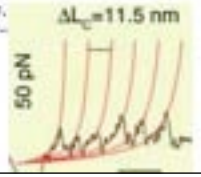

The I65-70 Six Domain Tandem of Titin

Available structure permits simulation of soft (tertiary structure) elasticity of titin.

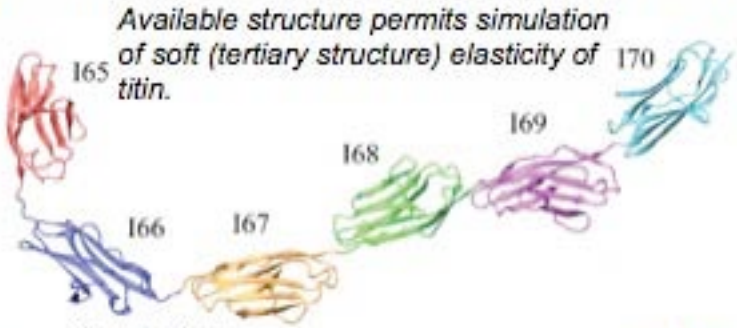

Structure from:
von Castelmur, E., M. Marino, D. I. Svergun, L. Kreplak, Z. Ucurum-Fotiadis, P. V. Konarev, A. Urzhumtsev, D. Labeit, S. Labeit, and O. Mayans.
Proc. Natl. Acad. Sci. USA. 105:1186–1191(2008)

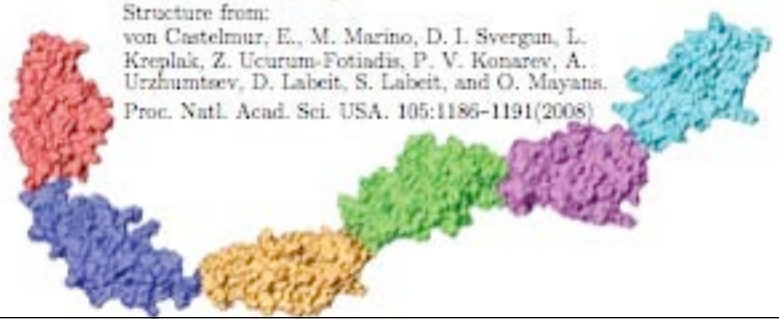

Stretching titin Ig6 (Ig65-Ig70) at low force

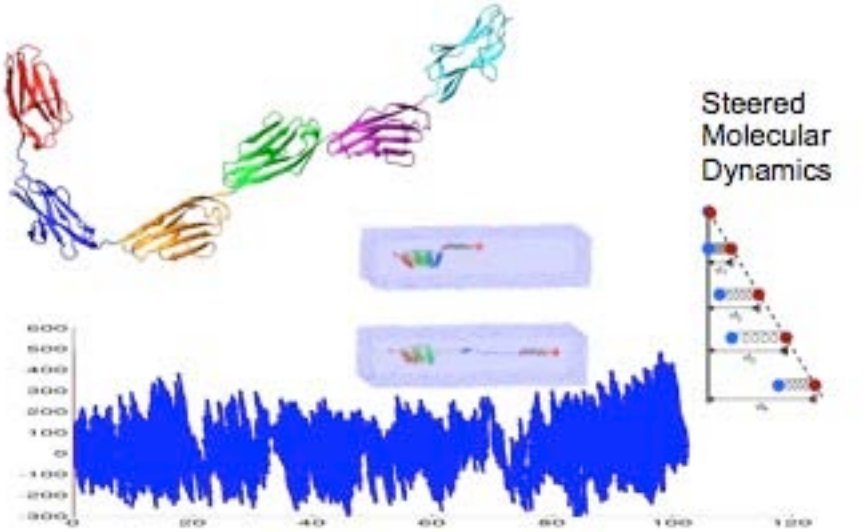

Stretching titin Ig6 (Ig65-Ig70) at low force

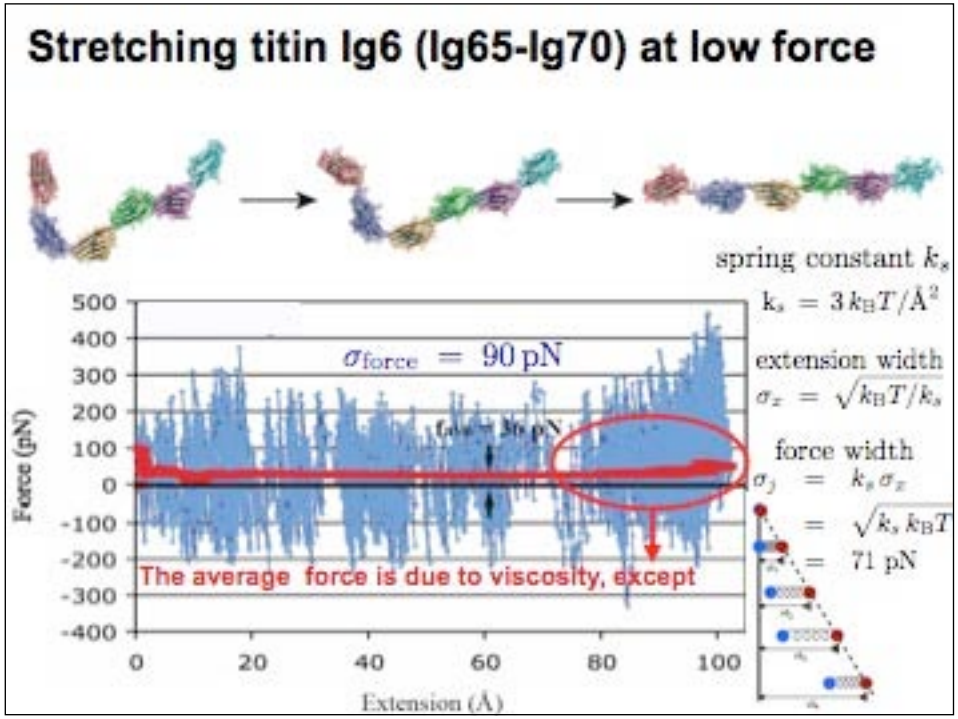

Secondary structure elasticity of titin Ig6

The simulation shows the stretching and rupturing of Ig6 one domain at a time, as seen in AFM experiments of $(I91)_N$ constructs.

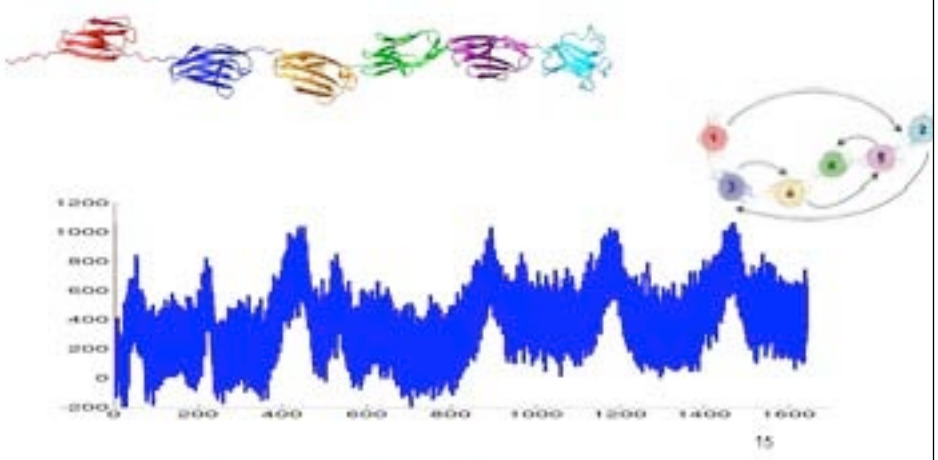

EH Lee, J Hain, E von Castelmur, O Mayans, and K. Schulten. Multidomain Elasticity of a Six-Ig Titin Chain. *in preparation*

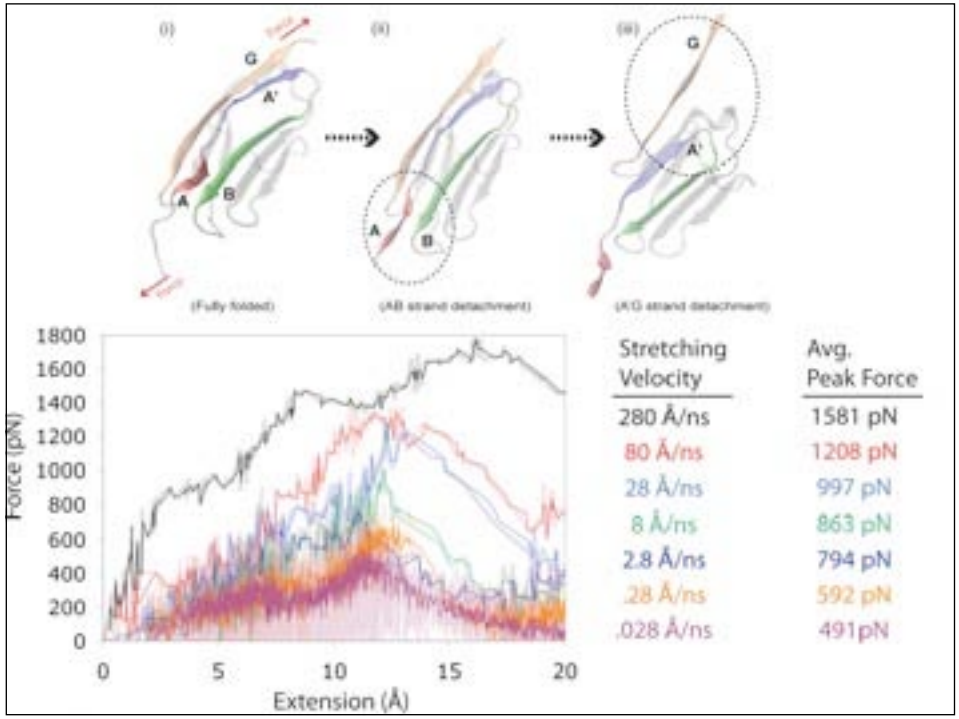

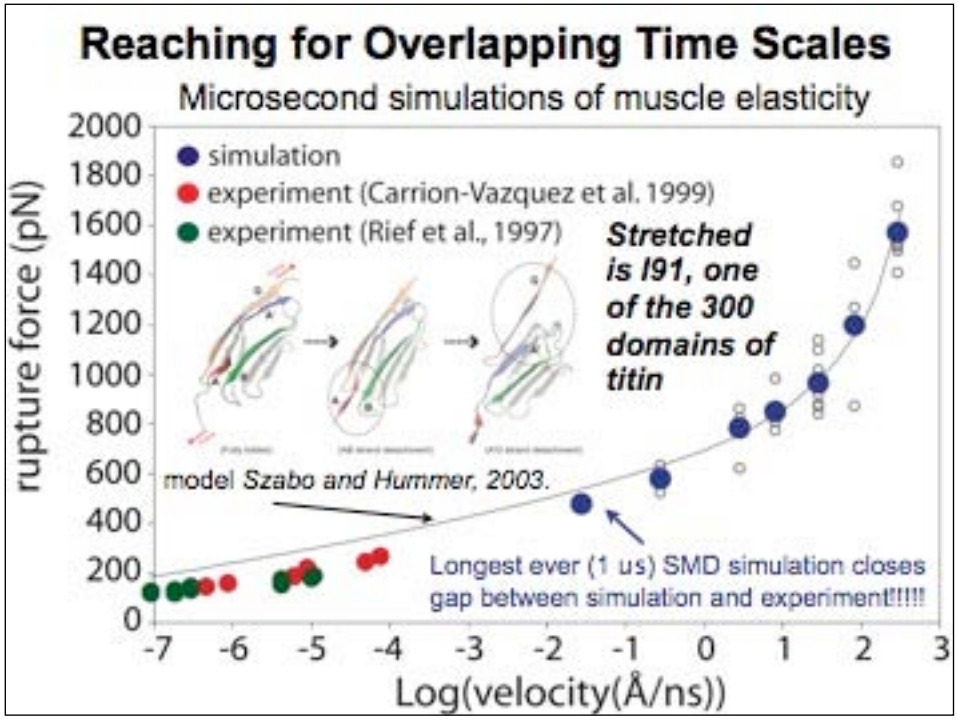
Reaching for Overlapping Time Scales
Microsecond simulations of muscle elasticity
simulation
experiment (Carrion-Vazquez et al. 1999)
experiment (Rief et al., 1997)
Stretched is I91, one of the 300 domains of titin
model Szabo and Hummer, 2003.
Longest ever (1 us) SMD simulation closes gap between simulation and experiment!!!!
rupture force (pN)
Log(velocity(Å/ns))

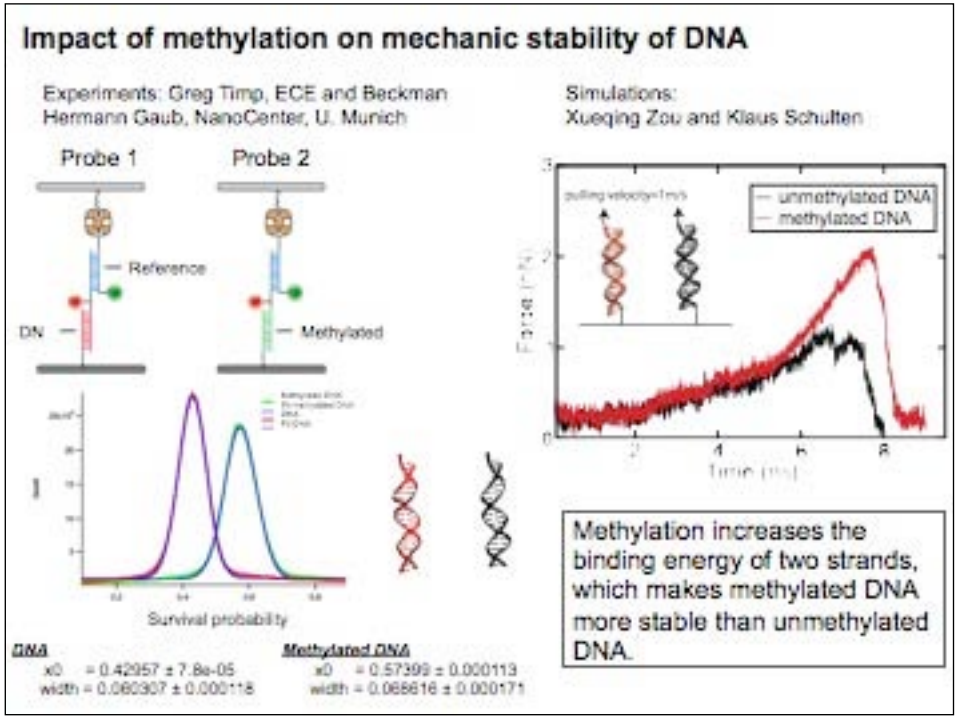
Impact of methylation on mechanic stability of DNA
Experiments: Greg Timp, ECE and Beckman
Hermann Gaub, NanoCenter, U. Munich
Simulations:
Xueqing Zou and Klaus Schulten
Probe 1
Probe 2
Reference
Methylated
unmethylated DNA
methylated DNA
Survival probability
DNA
x0 = 0.42957 ± 7.8e-05
width = 0.060307 ± 0.000118
Methylated DNA
x0 = 0.57399 ± 0.000113
width = 0.066616 ± 0.000171
Methylation increases the binding energy of two strands, which makes methylated DNA more stable than unmethylated DNA.

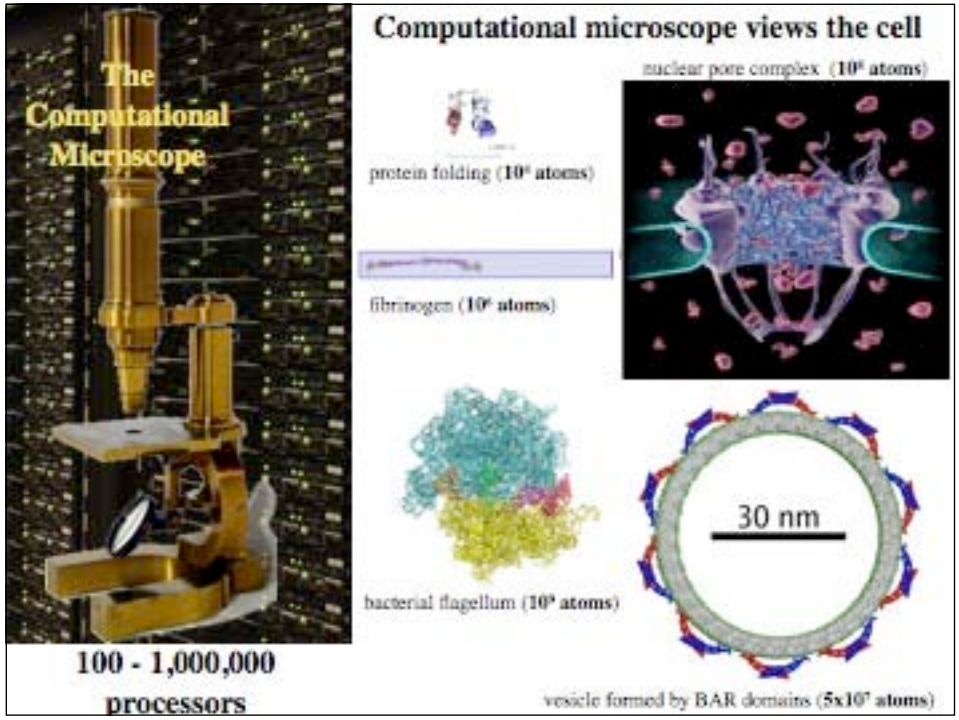
The Computational Microscope
Computational microscope views the cell
nuclear pore complex (10⁸ atoms)
protein folding (10⁴ atoms)
fibrinogen (10⁶ atoms)
30 nm
bacterial flagellum (10⁸ atoms)
100 - 1,000,000 processors
vesicle formed by BAR domains (5x10⁷ atoms)

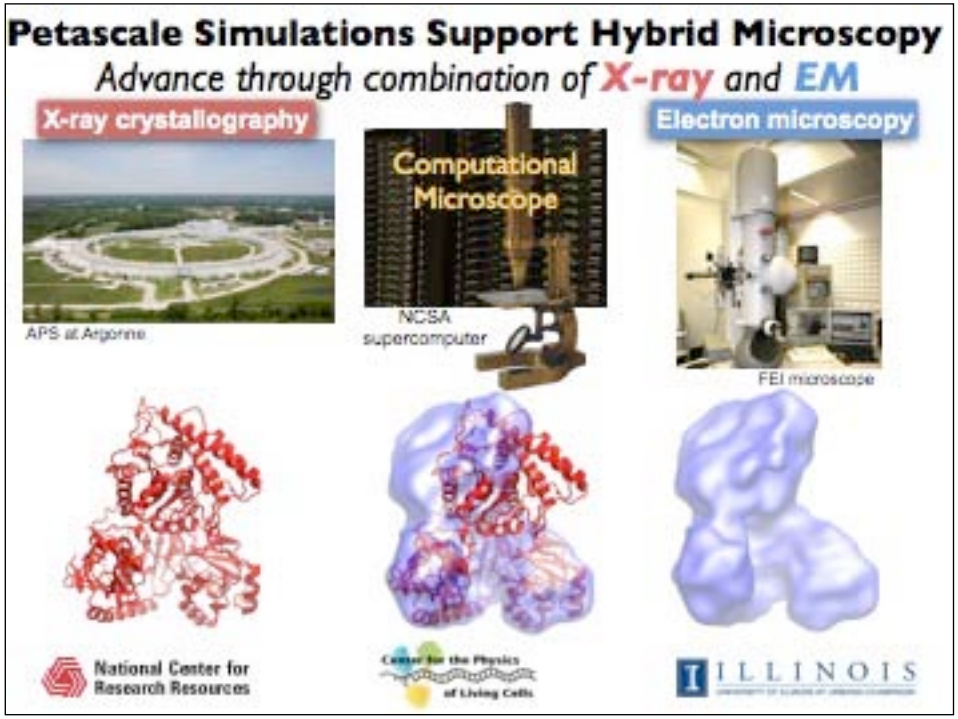
Petascale Simulations Support Hybrid Microscopy
Advance through combination of X-ray and EM
X-ray crystallography
Computational Microscope
Electron microscopy
APS at Argonne
NCSA supercomputer
FEI microscope
National Center for Research Resources
ILLINOIS

Molecular Dynamics Flexible Fitting with NAMD

Simulated ribosome system

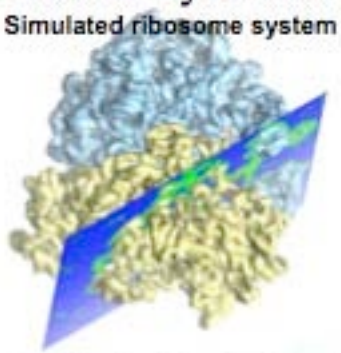

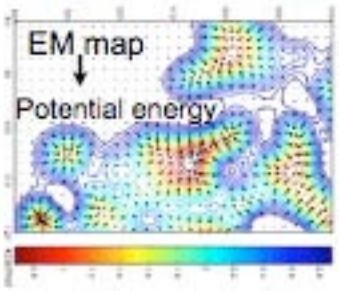

Performance on NCSA Abe

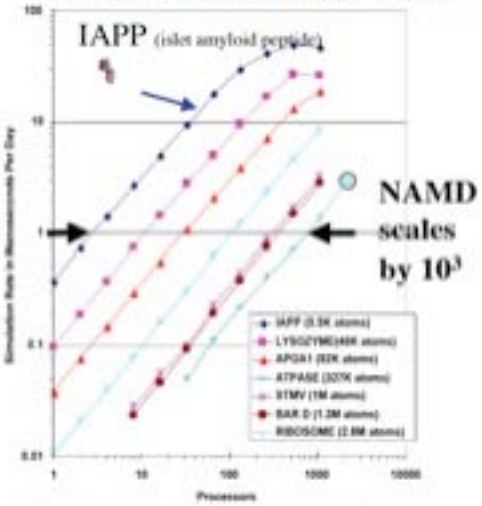

L. Trabuco, E Villa, K. Mitra, J. Frank, and K. Schulten. **Flexible fitting of atomic structures into electron microscopy maps using molecular dynamics.** *Structure*, 16:673-683, 2008.

Molecular Dynamics Flexible Fitting with NAMD

NAMD is a molecular dynamics program running efficiently on single processors up to thousands of processors; achieves 100 ns / day speed on 1K - 1 million K systems; available at all NSF-DOE centers in the US and worldwide; free to download

Simulated ribosome system

Performance on NCSA Abe

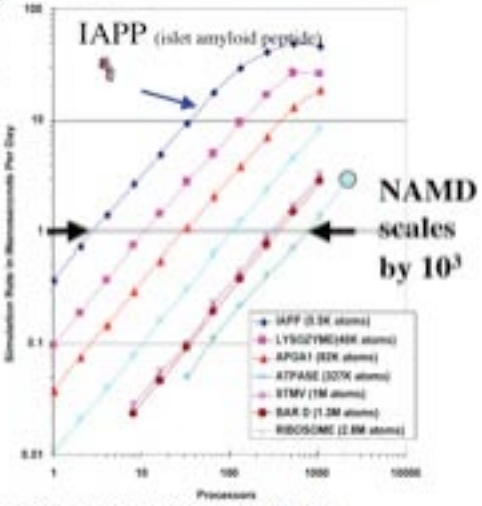

L. Trabuco, E Villa, K. Mitra, J. Frank, and K. Schulten. **Flexible fitting of atomic structures into electron microscopy maps using molecular dynamics.** *Structure*, 16:673-683, 2008.

Discovery Through the Computational Microscope

Gating mechanism of protein synthesis by the ribosome as key proofreading step after codon recognition

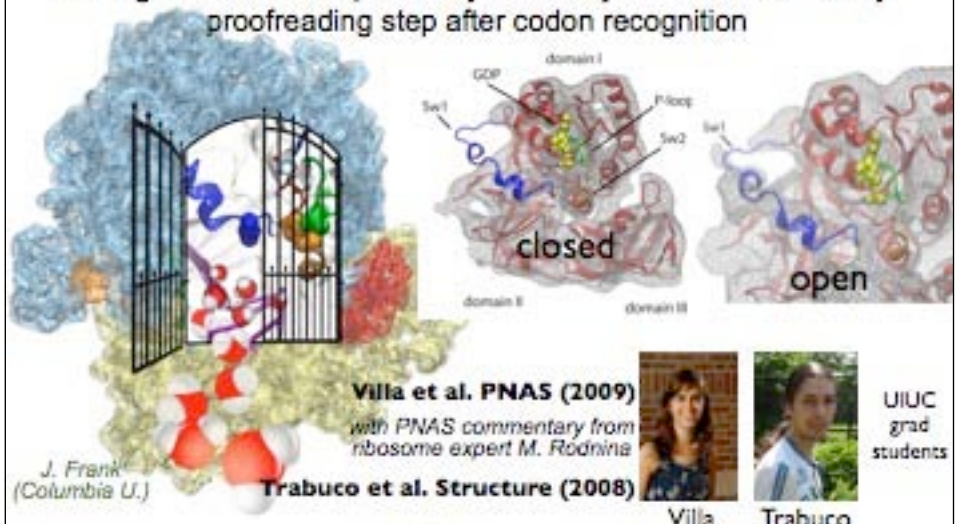

J. Frank (Columbia U.)

Villa et al. PNAS (2009)
with PNAS commentary from ribosome expert M. Rodnina

Trabuco et al. Structure (2008)

Villa

Trabuco

UIUC grad students

National Center for Research Resources

Center for the Physics of Living Cells

ILLINOIS

Successes of Computational Microscope Prototype

Gating mechanism of protein synthesis by the ribosome as key proofreading step after codon recognition

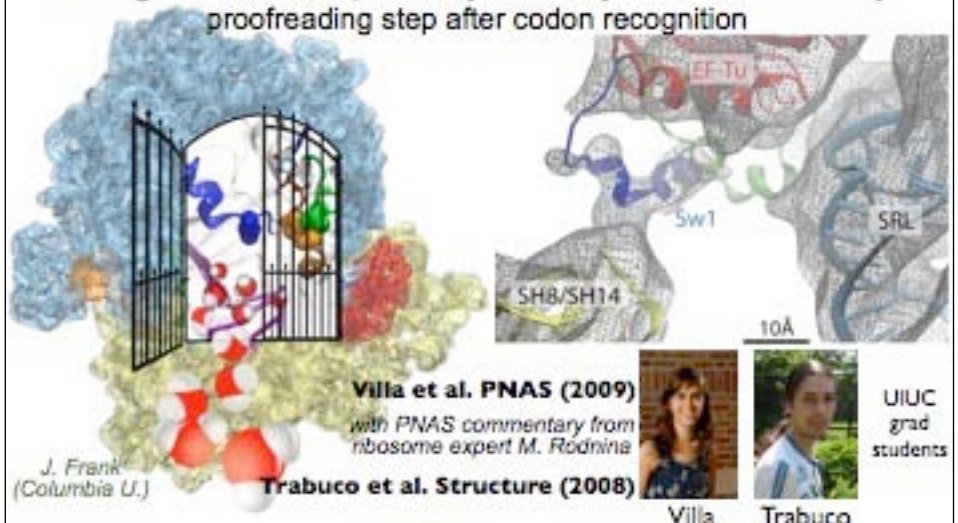

J. Frank (Columbia U.)

Villa et al. PNAS (2009)
with PNAS commentary from ribosome expert M. Rodnina

Trabuco et al. Structure (2008)

Villa

Trabuco

UIUC grad students

National Center for Research Resources

Center for the Physics of Living Cells

ILLINOIS

Modeling a ribosome-channel complex

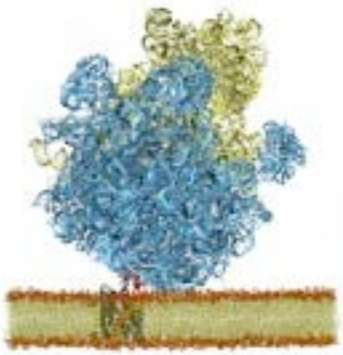

- Ribosome-SecY channel complex: known only from low-resolution density maps (grey outline)
- Used MD Flexible Fitting to fit atomic structures to map

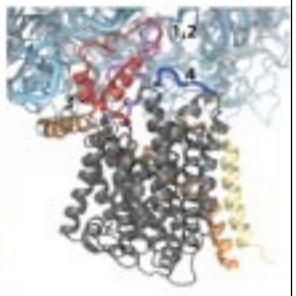

Simulation system
2.7 million atoms
simulated in total for nearly 50 ns

Simulations reveal atomic-scale interactions that maintain complex

Modeling a ribosome-channel complex

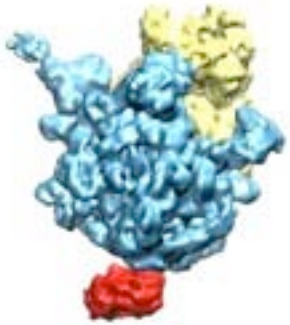

- Ribosome-SecY channel complex: known only from low-resolution density maps (grey outline)
- Used MD Flexible Fitting to fit atomic structures to map

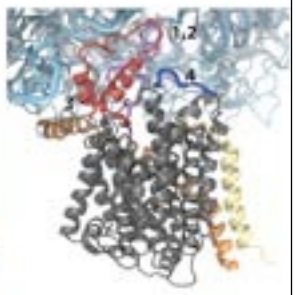

Simulation system
2.7 million atoms
simulated in total for nearly 50 ns

Simulations reveal atomic-scale interactions that maintain complex

Modeling a ribosome-channel complex

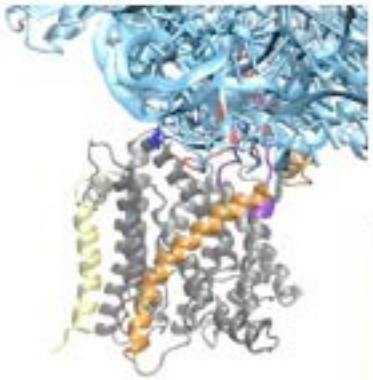

- Ribosome-SecY channel complex: known only from low-resolution density maps (grey outline)
- Used MD Flexible Fitting to fit atomic structures to map

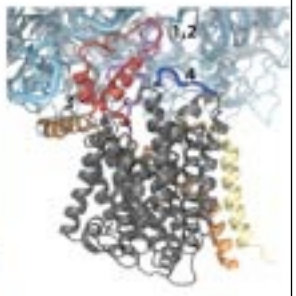

Simulation system
2.7 million atoms
simulated in total for nearly 50 ns

Simulations reveal atomic-scale interactions that maintain complex

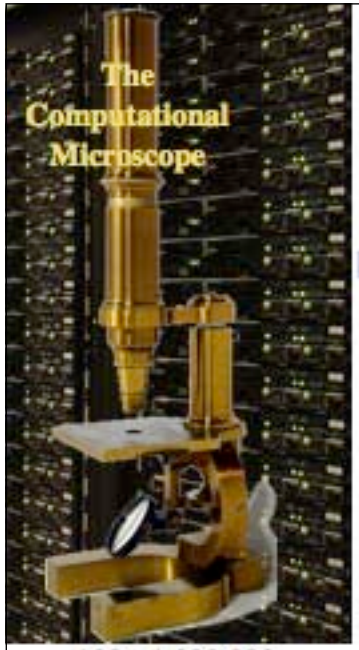

100 - 1,000,000 processors

Computational microscope views the cell

protein folding (10^5 atoms)

fibrinogen (10^6 atoms)

bacterial flagellum (10^8 atoms)

nuclear pore complex (10^8 atoms)

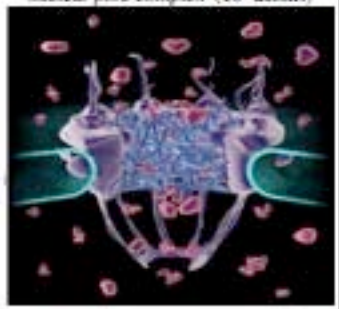

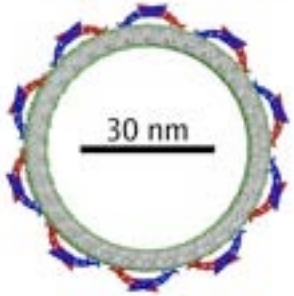

vesicle formed by BAR domains ($5x10^7$ atoms)

The Nuclear Pore Complex - What Is It?

NPC

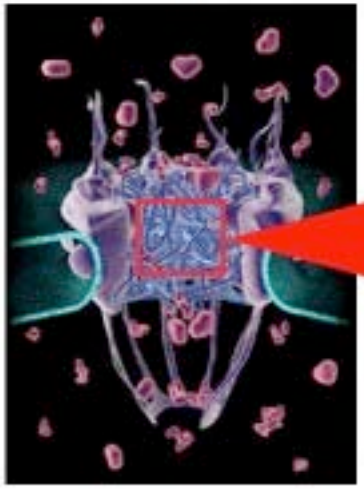

Section to be studied by molecular dynamics

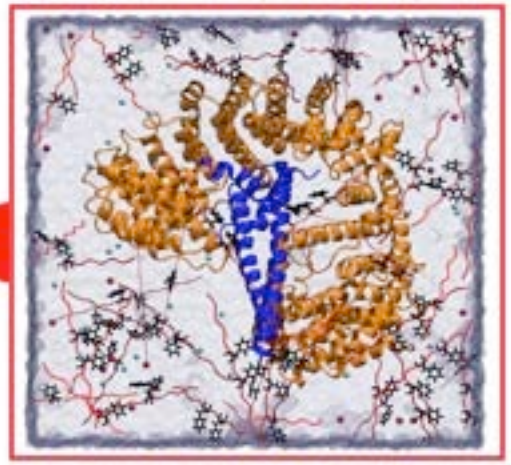

Importin-β; SREBP-2 cargo

transcription factor

Sampling of FG-nup Binding

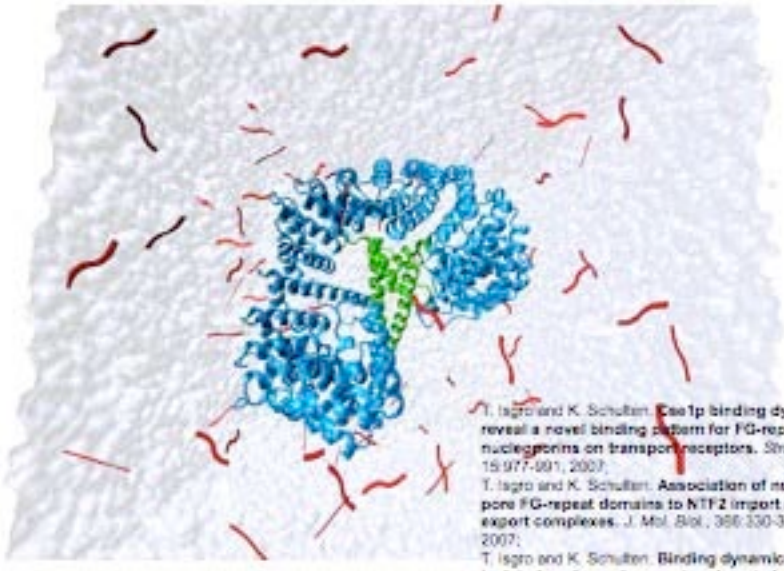

T. Isgro and K. Schulten. **Cse1p binding dynamics reveal a novel binding platform for FG-repeat nucleoporins on transport receptors.** *Structure*, 15:977-991, 2007;
T. Isgro and K. Schulten. **Association of nuclear pore FG-repeat domains to NTF2 import and export complexes.** *J. Mol. Biol.*, 366:330-345, 2007;
T. Isgro and K. Schulten. **Binding dynamics of isolated nucleoporin repeat regions to importin-β.** *Structure*, 13:1869-1879, 2005.

FG-nup Binding Pattern

How does the NPC distinguish between transport receptors and inert macromolecules?

- Any macromolecule may have random FG-nup binding spots
- Transport receptors exhibit a *particular* surface binding spot *pattern*
  - *Binding spots tend to be clustered with a ~14 Å spacing between spots*

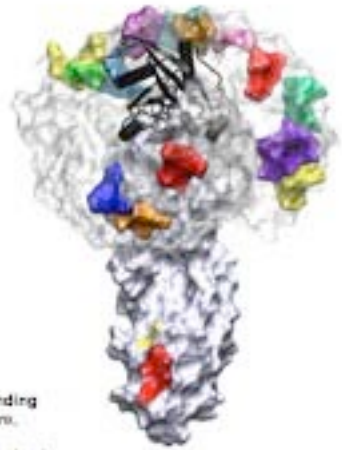

T. Iagro and K. Schulten. **Cse1p binding dynamics reveal a novel binding pattern for FG-repeat nucleoporins on transport receptors.** *Structure*, 15:977-991, 2007;
T. Iagro and K. Schulten. **Association of nuclear pore FG-repeat domains to NTF2 import and export complexes.** *J. Mol. Biol.*, 366:330-345, 2007;
T. Iagro and K. Schulten. **Binding dynamics of isolated nucleoporin repeat regions to importin-β.** *Structure*, 13:1669-1679, 2005.

Residue-based coarse-graining

J. Phys. Chem. B, 110:3674-3684, 2006

Transport-related structures and processes of the nuclear pore complex studied through molecular dynamics. *Structure*, 17:449-459, 2009

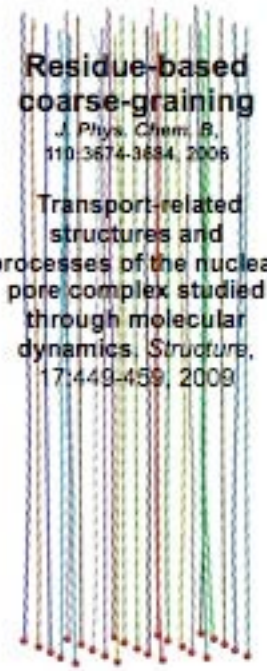

Simulating an Array of Nsp1 Segments Tethered to a Planar Lattice at NPC Density Coarse-Grained

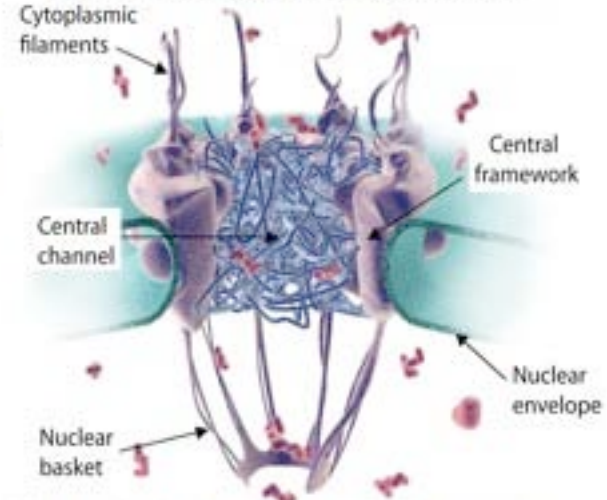

FG-Nup coiling into bundled, netted brushes, revealing the structure of the gel-like gate.

FG-Nup coiling into bundled, netted brushes, revealing the structure of the gel-like gate.

Using the Prior Coarse-Grained Simulation, Reverse Coarse Graining Permits One to Explore at Atomic Level Structure and Dynamics

The Computational Microscope Reveals the NPC Selective Barrier Structure?

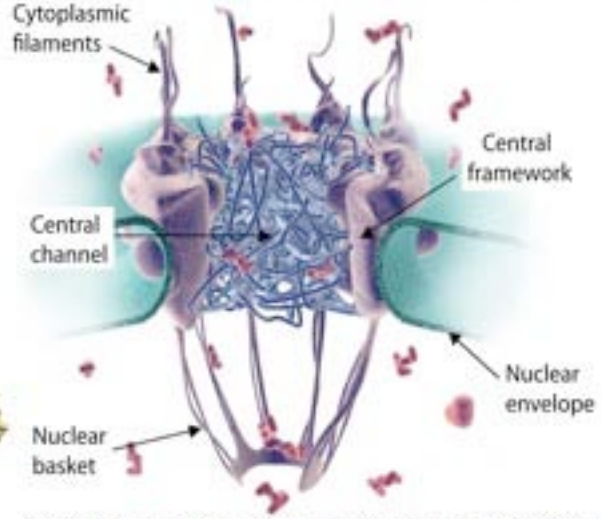

T. Ando and K. Schulten, **Cse1p binding dynamics reveal a novel binding pattern for FG-repeat nucleoporins on transport receptors.** *Structure*, 15:977-991, 2007. **Association of nuclear pore FG-repeat domains to NTF2 import and export complexes.** *J. Mol. Biol.*, 366:330-345, 2007; **Binding dynamics of isolated nucleoporin repeat regions to importin-β.** *Structure*, 13:1868-1879, 2005.

L. Miao and K. Schulten, **Transport-related structures and processes of the nuclear pore complex studied through molecular dynamics.** *Structure*, 17:449-459, 2009

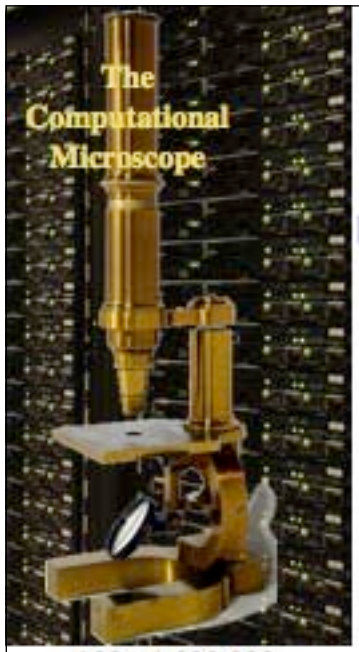

100 - 1,000,000 processors

Computational microscope views the cell

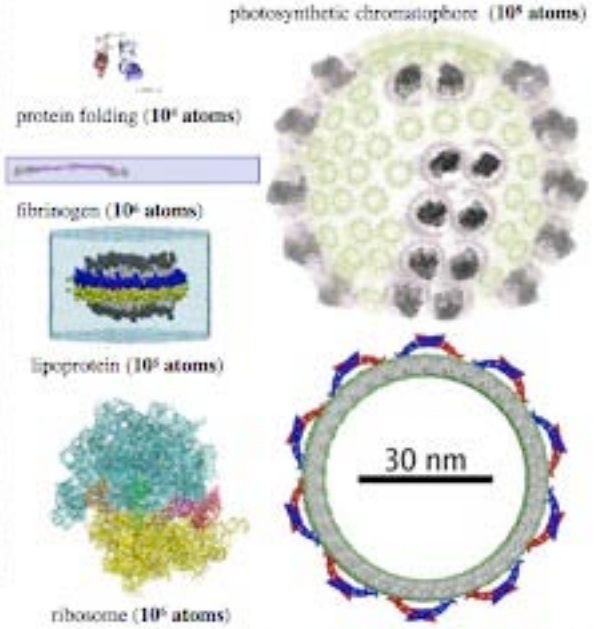

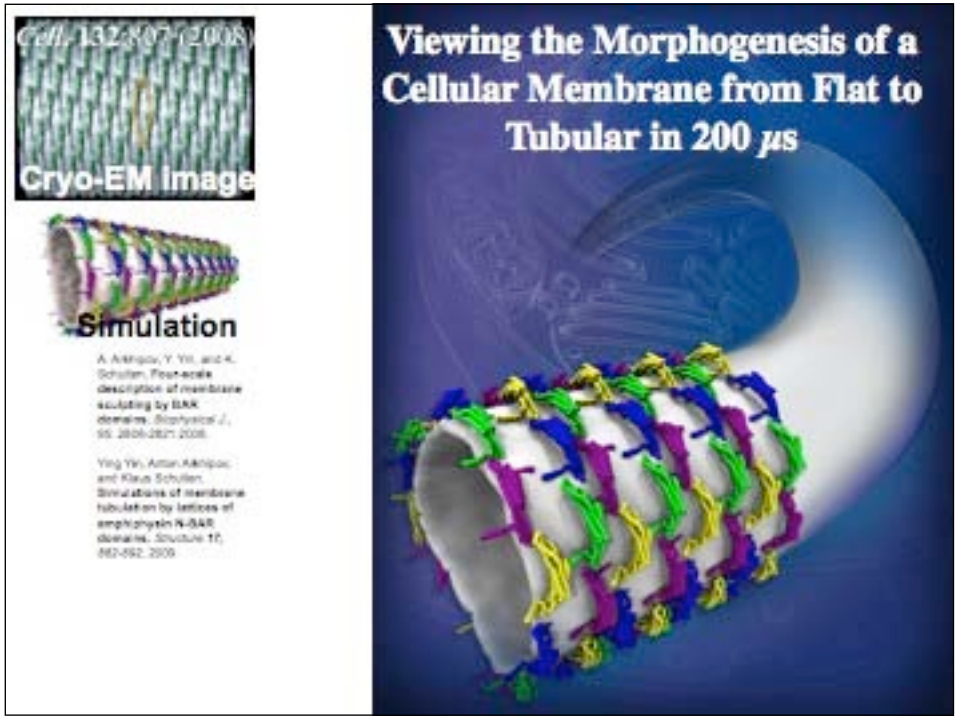
Cryo-EM image
Simulation
Viewing the Morphogenesis of a Cellular Membrane from Flat to Tubular in 200 μs

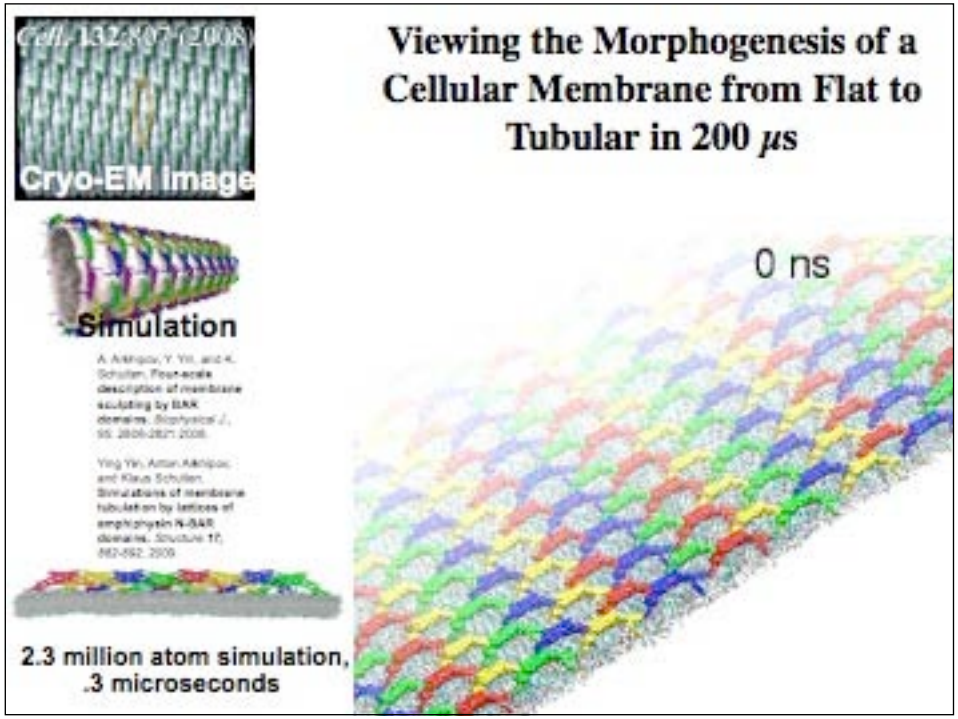
Cryo-EM image
Simulation
Viewing the Morphogenesis of a Cellular Membrane from Flat to Tubular in 200 μs
0 ns
2.3 million atom simulation,
.3 microseconds

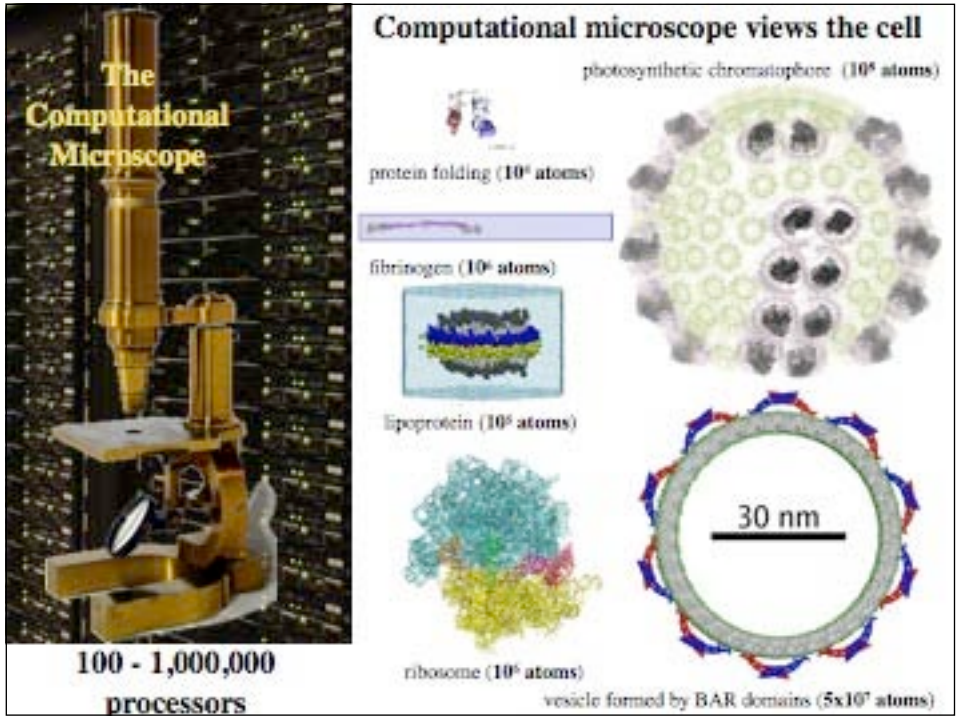
The Computational Microscope
100 - 1,000,000 processors
Computational microscope views the cell
photosynthetic chromatophore (10⁸ atoms)
protein folding (10⁴ atoms)
fibrinogen (10⁵ atoms)
lipoprotein (10⁶ atoms)
ribosome (10⁶ atoms)
30 nm
vesicle formed by BAR domains (5x10⁷ atoms)

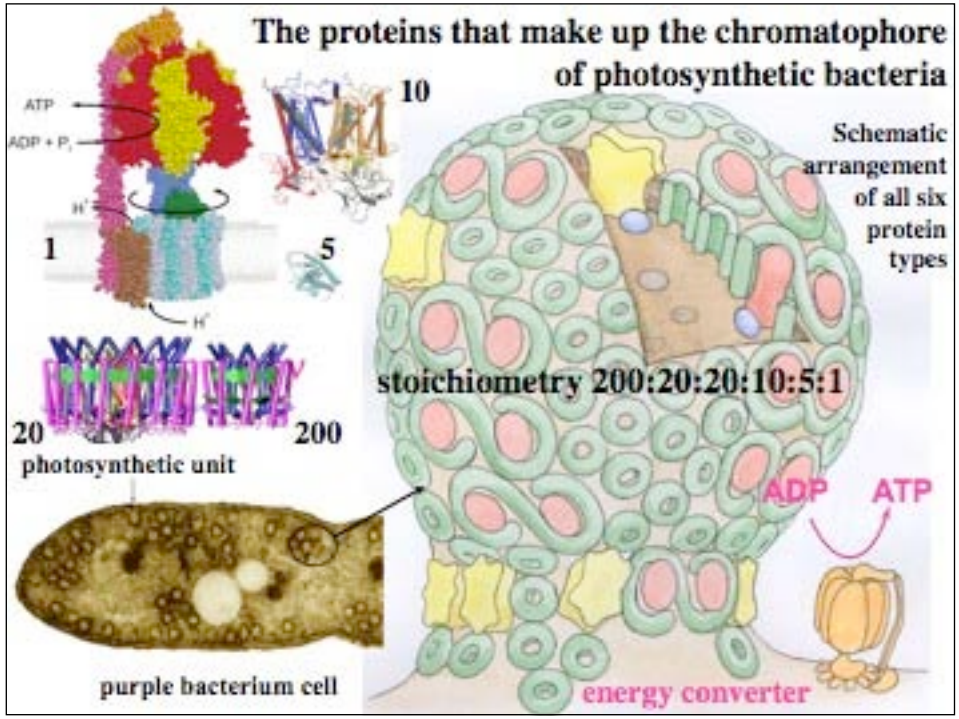
The proteins that make up the chromatophore of photosynthetic bacteria
ATP
ADP + Pi
H+
1
10
5
20
200
photosynthetic unit
purple bacterium cell
Schematic arrangement of all six protein types
stoichiometry 200:20:20:10:5:1
ADP
ATP
energy converter

Chromatophore of Purple Bacteria

(section of the chromatophore membrane)

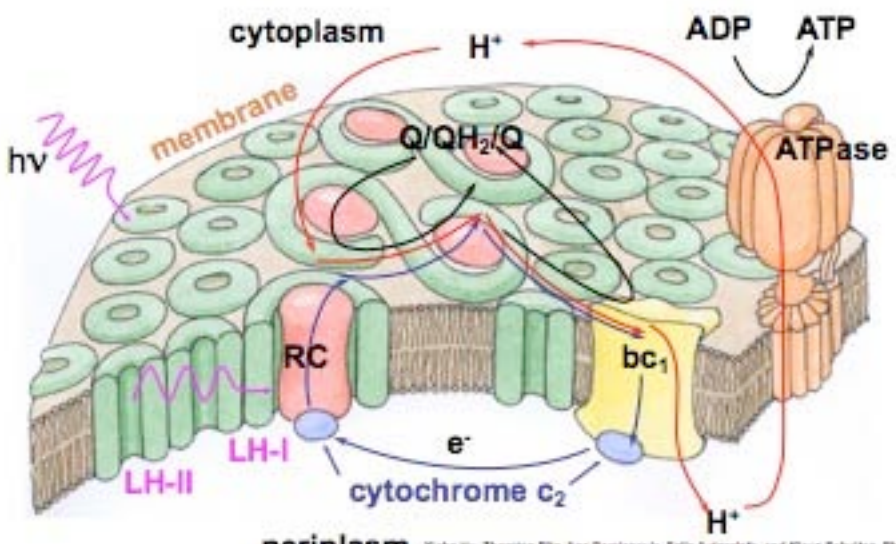

Xiche Hu, Thorsten Ritz, Ana Damjanovic, Felix Autenrieth, and Klaus Schulten. Photosynthetic apparatus of purple bacteria. Quarterly Reviews of Biophysics, 35:1-62, 2002.

Component 1: Light Harvesting Complex 2 (LH2)

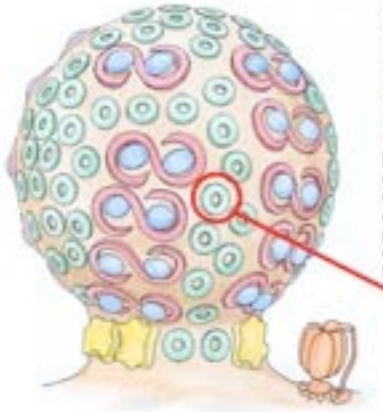

- LH2 absorbs light via its bacteriochlorophylls (below in Green)
- This energy is transferred to the LH1 where the reaction center utilizes it to pump electrons across the membrane
- LH2 complexes form the bulk of chromatophore membranes and are integral to both its structure and function

Danielle Chandler, Jen Hsin, Christopher B. Harrison, James Gumbart, and Klaus Schulten. **Intrinsic curvature properties of photosynthetic proteins in chromatophores.** *Biophysical Journal*, 95:2822-2836, 2008.

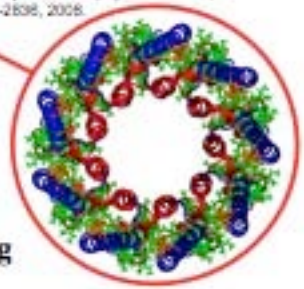

Structure of LH2 established by crystallography & homology modeling

LH2

LH2 aggregates induce curvature via packing

7 hexagonally-packed LH2s

"packed" → no lipids between LH2s

"sparse" → one layer of lipids between LH2s

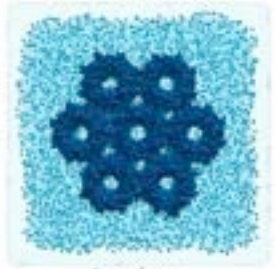

top view

side view after 12 ns

"packed" vs. "sparse"

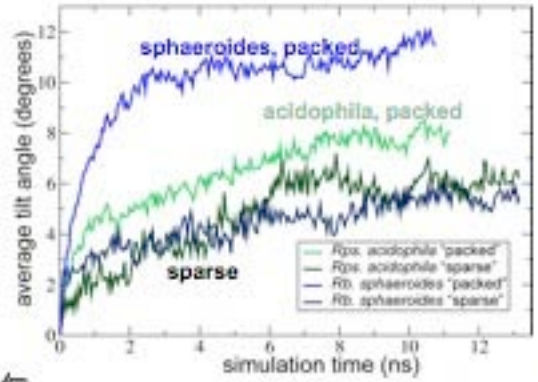

LH2 curvature partially driven by electrostatics

curvature is reduced by removal of conserved cytoplasmic charged residues

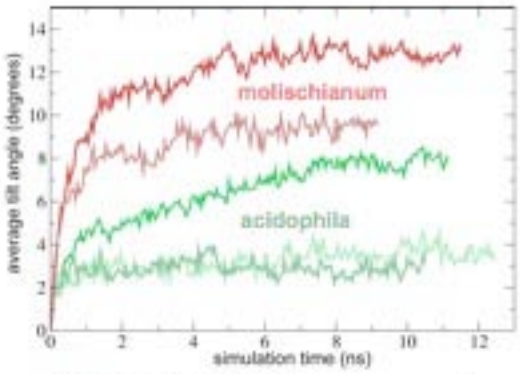

Ph. molischianum wild-type

Ph. molischianum modified

Much reduced curvature in LH1-LH2 mixed system

LH1 monomer surrounded by seven LH2 complexes

(LH1 and LH2 from *Rps. acidophila*, RC from *Rb. sphaeroides*)

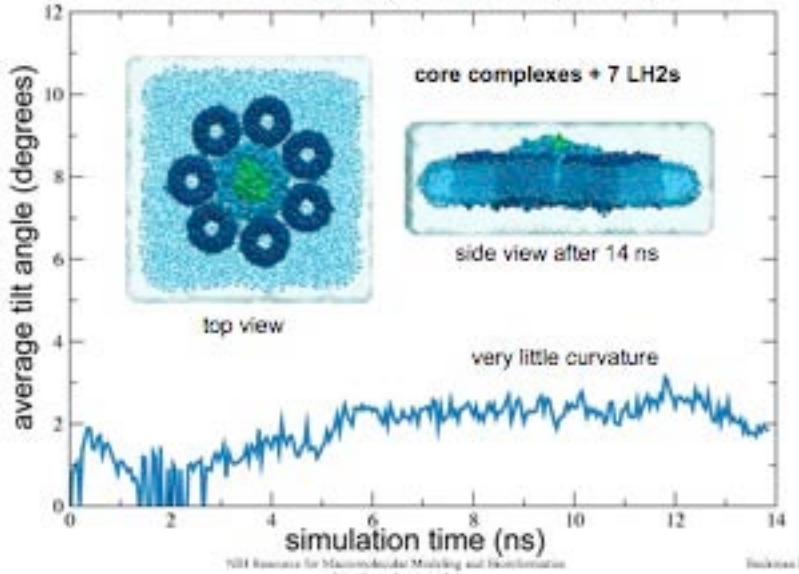

Component 2: Light Harvesting Complex 1 (LH1)

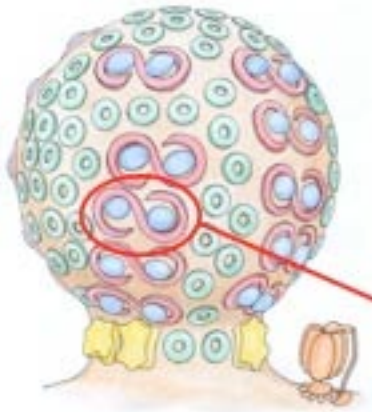

- LHIs form stacks in spherical chromatophores
- LH1 is dimeric multi-protein complex of
  - Light Harvesting Complex 1 (LH1) (Blue & Red)
  - Reaction Center (RC) (Green)
  - Puf X (Purple)
- LH1 absorbs light energy, transfers it to RC which uses it to pump electrons across the membrane.

Jen Hsin, James Gumbart, Leonardo G. Trabuco, Elizabeth Villa, Pu Qian, C. Neil Hunter, and Klaus Schulten, **Protein-induced membrane curvature investigated through molecular dynamics flexible fitting**, *Biophysical Journal*, 2009. In press.

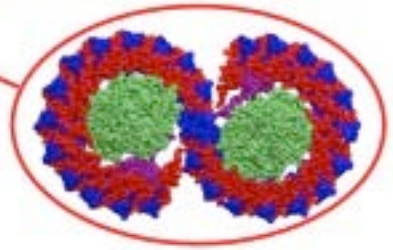

Structure of LH1 established through crystallography and model-fitting to EM densities

LH1

All-atom Simulations of a Membrane-Bending Protein Complex

Top View

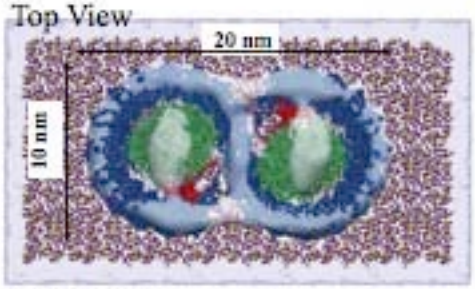

Side View

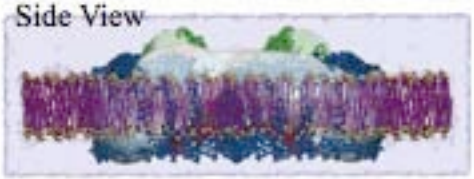

Photosynthetic core complex:

0.9 million atoms

simulated in total for > 51 ns

- Core complex stacks into tubes in bacterial cells
- Each core complex is thought to induce local curvautre in membrane

Sener et al., *Chem. Phys.* 357:188-197 (2009)
Hsin et al., *Biophys. J.*, in press (2009)

All-atom Simulations of a Membrane-Bending Protein Complex

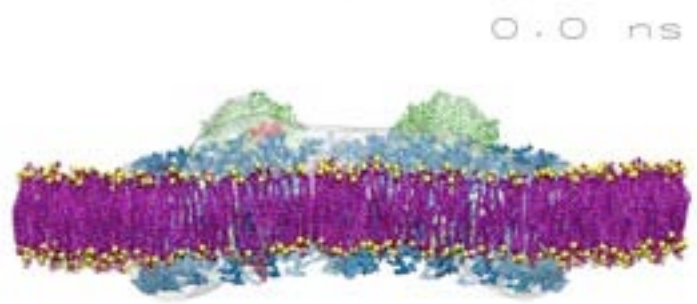

- Simulations revealed the membrane-bending process
- Size of the membrane curvature matched that of experiment
- Local curvature is related to long-range organization of the complex

Sener et al., *Chem. Phys.* 357:188-197 (2009)
Hsin et al., *Biophys. J.*, in press (2009)

Knowing the Atomic Level Structure of the chromatophore, one can systematically describe its physical mechanism

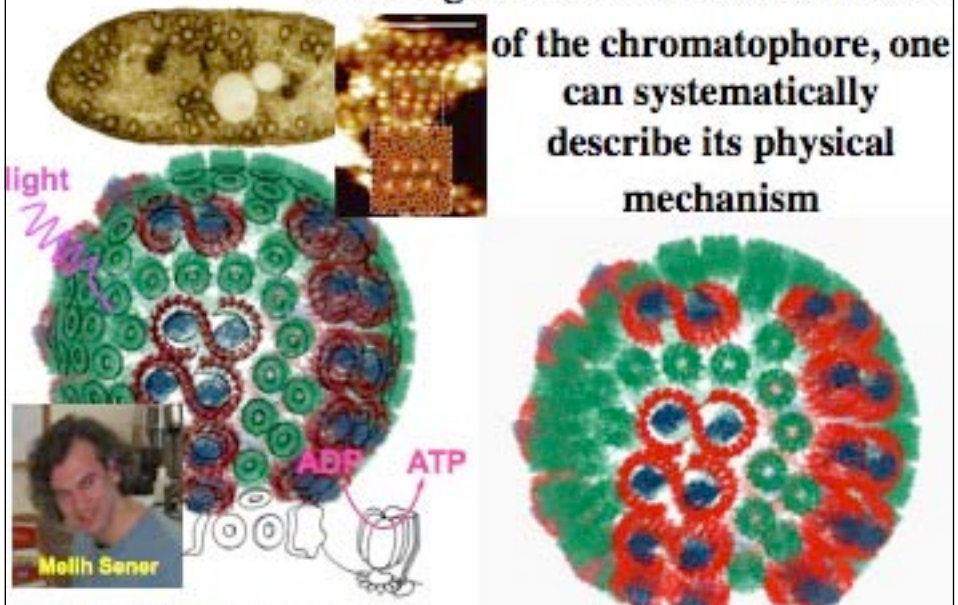

M. Sener, J. Olsen, N. Hunter, and K. Schulten. *PNAS*, **104:** 15723-15728, 2007

The "Physics" of Light Harvesting in the Chromatophore

Calculated Energy Transfer Rates Determine Optimal Placement of Proteins in Chromatophore

$$W_{jk} = C\left(\frac{\vec{d}_j \cdot \vec{d}_k}{r_{jk}^3} - \frac{3(\vec{r}_{jk} \cdot \vec{d}_j)\,(\vec{r}_{jk} \cdot \vec{d}_k)}{r_{jk}^5}\right)$$ links: induced dipole - induced dipole interaction

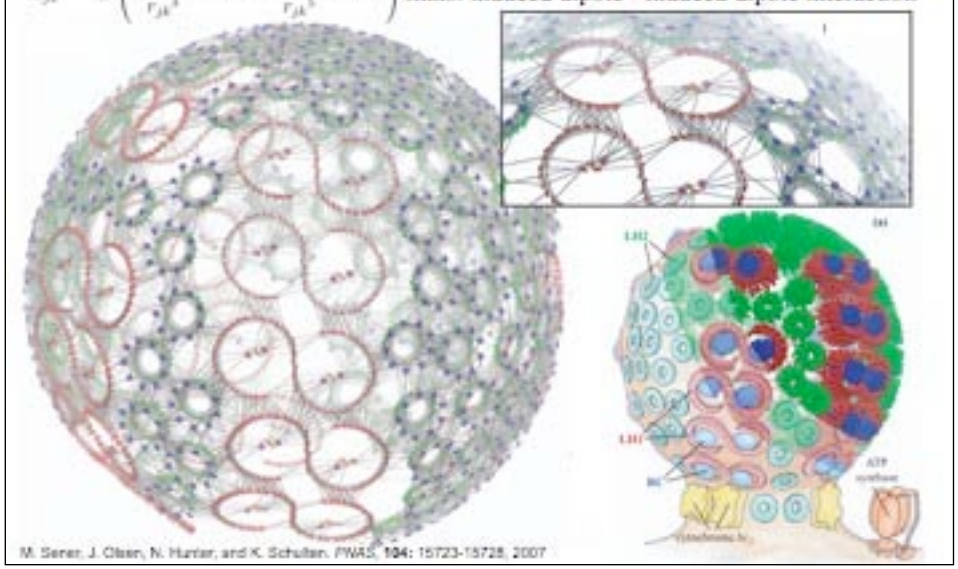

M. Sener, J. Olsen, N. Hunter, and K. Schulten. *PNAS*, **104:** 15723-15728, 2007

The "Physics" of Light Harvesting in the Chromatophore

$$W_{jk} = C\left(\frac{\vec{d}_j \cdot \vec{d}_k}{r_{jk}^3} - \frac{3(\vec{r}_{jk} \cdot \vec{d}_j)\,(\vec{r}_{jk} \cdot \vec{d}_k)}{r_{jk}^5}\right)$$

links: induced dipole - induced dipole interaction

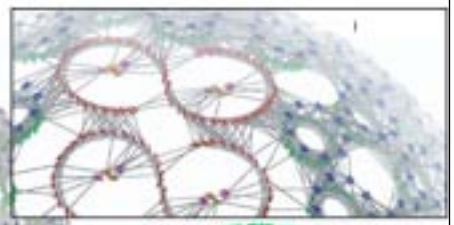

rate equation

$$\partial_t |p(t)\rangle = K|p(t)\rangle$$

$$q_j = \int_0^\infty dt\, k_{et}\langle \mathrm{RC}|p(t)\rangle = -k_{et}\langle \mathrm{RC}|K^{-1}|e_j\rangle$$

$$t_j = \int_0^\infty dt\, k_{loss}\langle e_j|p(t)\rangle = -k_{loss}\langle e_j|K^{-1}\frac{1}{N}|1\rangle$$

$$\tau_j = \int_0^\infty dt\, \langle 1|p(t)\rangle = -\langle 1|K^{-1}|e_j\rangle$$

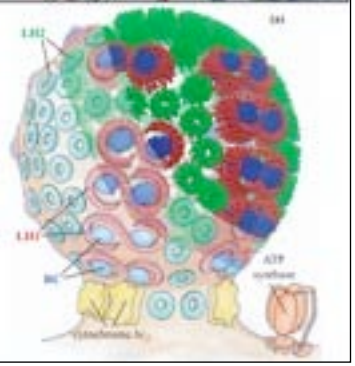

Form-follows-function architecture of purple bacterial light harvesting systems

Klaus Schulten, Jen Hsin, Danielle Chandler, Melih Sener
U. Illinois at Urbana-Champaign

Collaborators: Neil Hunter, Arvi Freiberg, Tony Crofts, Chris Chipot

Acknowledgements

NAMD leaders
L. Kale
J. Phillips
S. Kumar (IBM)

polarizable ff
P. Freddolino
D. Hardy

fibrinogen
E. Lee
B. Lim (Mayo)

10 μs folding
P. Freddolino
M. Gruebele (UIUC)

BAR domain
Y. Yin
A. Arkhipov

GPU team
J. Stone (leader)
D. Hardy
B. Isralewitz
J. Saam
K. Vandivoort
R. Brunner
W. Hwu (UIUC leader)

ribosome
Elizabeth Villa
L. Trabuco
J. Gumbart
J. Frank (Columbia U.)

nuclear pore complex
T. Isgro
L. Miao

Funding: NIH, NSF

National Center for Research Resources

DOE - Incite